Preparation and properties of rapeseed straw based porous carbon materials

Sha Yan[1†], Siyu Hu[1,2†], Qinyu Yang[1,2], Ting Guo[1,2], Xinxin Zhao[1,2], Meng Wang[1,2], Zuoping Zhao[1,2*]

(1. *School of Mathematics and Computer Science, Shaanxi University of Technology, Hanzhong 723001, Shaanxi, China*;
2. *State Key Laboratory of Qinba Bio-Resource and Ecological Environment, Hanzhong 723001, Shaanxi, China*)

Abstract: The conversion of rapeseed straw into biochar not only effectively mitigates pollution from traditional straw burning but also aligns with China's sustainable agricultural development goals. A significant quantity of rapeseed stalks is frequently burned in fields, leading to severe air pollution characterized by black smoke and residue, resulting in a substantial waste of straw resources. To address this issue, rapeseed straw form Nanchi Village, Puzhen Town, Hanzhong City, Shaanxi Province, China was utilized as a precursor and KOH was employed as an activator to produce porous activated carbon by pyrolysis. Scanning electron microscopy (SEM), elemental analyzer, infrared spectroscopy, specific surface area analysis, and other instruments were employed to characterize the porous activated carbon produced under various temperature gradients and activator concentrations. The microelement composition, structure, specific surface area, and pore size of biochar produced under varying conditions were analyzed to determine the optimal preparation parameters. Furthermore, the adsorption efficiency for tetracycline in wastewater was evaluated using a three-factor, three-level orthogonal experimental design. The results showed that the interior of the activated carbon was porous, while the exterior contained oxygenated functional groups that facilitated the adsorption of nitrogen, phosphorus, and other elements. The optimal carbonization temperature and KOH concentration for activated carbon were determined to be 400°C and 0.5, respectively. The optimal adsorption conditions were identified as pH value of 7, an initial tetracycline concentration of 30 mg/L, a biochar dosage of 0.2 g, an adsorption time of 60 min, and a removal rate of 98.53%. The factors influencing the adsorption of tetracycline onto rapeseed straw biochar were ranked as initial tetracycline concentration>adsorption reaction time>biochar dasage. The findings will provide valuable references for research on biochar performance and the treatment of tetracycline contamination in water.

Keywords: rapeseed straw, biochar, preparation, characterization, adsorption

DOI: 10.25165/j.ijabe.20241705.8882

Citation: Yan S, Hu S Y, Yang Q Y, Guo T, Zhao X X, Wang M, et al. Preparation and properties of rapeseed straw based porous carbon materials. Int J Agric & Biol Eng, 2024; 17(5): 120–127.

1 Introduction

With the progress of society and the development of science and technology, the issue of ecological environmental protection has become increasingly prominent. Among these concerns, industrial wastewater discharge has severely polluted surface water, while the indiscriminate use of pesticides in agriculture has introduced a significant amount of pollutants[1]. The discharge of various pollutants leads to significant deterioration of surface water quality over large areas, consequently exacerbating the problem of water scarcity[2,3]. Tetracycline (TCs) is one of the most widely abundant antibiotics in contaminants.

According to statistics, in 2013, the annual consumption of TCs accounted for 46% (2300 t) of the total antibiotic consumption in the European Union, while in China, TCs represented 7% (12 000 t) of the total. The water system serves as one of the ultimate environmental reservoirs for antibiotics, with over 50% of TCs eventually entering aquatic systems through various pathways. Studies have shown that the maximum detected concentrations of TC, OTC, and CTC in the Yangtze River Basin were 11.60 ng/L, 18.98 ng/L, and 5.86 ng/L, respectively. Furthermore, the concentration of TCs in drinking water in the Huaihe River Basin ranged from 68.60 to 632.00 ng/L[4].

Tetracycline is challenging for organisms to absorb and metabolize and is eventually excreted through feces and urine, inevitably leading to significant environmental and ecological issues[5]. Additionally, tetracycline accumulates in groundwater, surface water, and soil, leading to bacterial drug resistance and posing potential threats to aquatic ecosystems. The indirect effects of this contamination also jeopardize the health of humans and other organisms[6]. Therefore, both for environmental protection and the long-term development of human civilization, the treatment and control of tetracycline in wastewater have become urgent tasks in contemporary environmental governance[7,8]. Various methods exist for the removal of tetracycline from wastewater, with traditional techniques including adsorption, the activated sludge process, and membrane separation technology[9]. Adsorption is an economical and effective method to mitigate tetracycline pollution, with the choice of adsorbent (e.g., carbon nanotubes, fly ash) being a critical

Received date: 2024-02-25 **Accepted date:** 2024-05-27

Biographies: **Sha Yan**, Lecturer, research interest: ecological mathematical model, Email: Yansha6688@126.com; **Siyu Hu**, MS, research interest: environmental pollution control, Email: 1430291298@qq.com; **Qinyu Yang**, MS, research interest: environmental pollution control, Email: 2298457183@qq.com; **Ting Guo**, PhD, Lecturer, research interest: environmental functional materials and water pollution control, Email: guotingjob@163.com; **Xinxin Zhao**, PhD, Lecturer, research interest: environmental pollution control, Email: zhaoxinxin@snut.edu.cn; **Meng Wang**, PhD, Lecturer, research interest: environmental functional materials and agricultural pollution control, Email: mwang303@163.com.

†contributed equally to this work

***Corresponding author: Zuoping Zhao**, PhD, Professor, research interest: environmental pollution control. College of Chemical and Environmental Sciences, Shaanxi University of Technology, Hanzhong 723001, Shaanxi, China. Tel: +86-13992691039, Email: zhaozuoping@126.com.

factor in its effectiveness. However, the high cost of these adsorbents, along with their potential for secondary pollution, significantly limits their application[10-14]. Recently, biochar has emerged as a promising and cost-effective adsorbent for tetracycline removal from wastewater, attracting significant scholarly attention due to its vast potential in environmental management and governance[15,16]. In recent years, considerable research has been conducted on the adsorption and removal of organic matter from water using biochar, as well as on its modification[17-21].

Zhang et al.[22] found that biochar is a solid product rich in carbon, highly aromatic, and stable, produced through the hydrolysis of biomass. It contains not only carbon but also hydrogen, nitrogen, sulfur, and oxygen, among other elements. Ash is one of the inorganic components. Structurally, biochar exhibits an uneven distribution of pores, including macropores, micropores, and mesopores. The specific surface area typically measures less than 400 m^2/g[23,24]. Due to its favorable physical and chemical characteristics, such as an abundant pore structure, large specific surface area, and numerous functional groups, rapeseed straw biochar is widely utilized in soil remediation, sewage treatment, and energy production[25]. Lan et al.[26] demonstrated that wastewater containing organic solutions causes significant environmental harm. Rapeseed straw biochar, being a porous and effective adsorbent, is widely employed in environmental protection, particularly in sewage purification. Li et al.[27] investigated the effect of biochar on tetracycline adsorption by preparing biochar from various straw-based materials. Their study revealed that rapeseed straw biochar exhibited superior adsorption capacity for tetracycline in organic solutions. Huang et al.[28] reported that the adsorption capacity of rapeseed straw biochar for tetracycline in organic wastewater reached up to 209.5922 mg/g.

Biochar is a widely utilized material. It exhibits low energy consumption and high removal efficiency while offering significant economic benefits, including cost reduction and enhanced resource utilization[29]. As an important renewable resource, rapeseed straw biochar facilitates the recycling of agricultural materials. On one hand, the production cost of biochar is low; on the other hand, incorporating rapeseed straw biochar into soil as an amendment enables the recycling of agricultural waste. The extensive secondary utilization of domestic waste transforms it into an environmentally friendly material, thereby enhancing its ecological value. During biochar production, the carbonization occurs in an oxygen-neutral environment, with the raw material powder maintained in a nitrogen atmosphere, thereby preventing secondary environmental pollution[30]. The gas produced can also be reused, consequently reducing the cost of biochar production. Although biochar adsorption and modification have been extensively studied, the optimal conditions for biochar preparation and the adsorption of tetracycline from wastewater have not been thoroughly investigated. In southern Shaanxi, the predominant farmland crop is rape, resulting in a substantial amount of straw after harvest. To effectively utilize resources and improve the water environment in southern Shaanxi, rape straw from the Hanzhong rape base was used as the precursor. Therefore, this study aims to employ indoor culture techniques, using tetracycline to simulate antibiotic wastewater, to investigate the effects of various factors—including biochar dosage, reaction time, pH, and initial antibiotic concentration-on the adsorption and removal of tetracycline. The findings will provide valuable references for research on biochar performance and the treatment of tetracycline contamination in water.

2 Materials and methods

2.1 Preparation of biochar

2.1.1 Pretreatment of matrix materials

The precursor used in this study is rape straw sourced from the rape base in Nanchi Village, Pu Town, Hanzhong City, Shaanxi Province, China. The rape straw was washed with distilled water to remove surface impurities, cut into small pieces, dried, and then placed in an oven at 108°C for 12 h.

2.1.2 Carbonization of biochar

The pretreated straw powder was weighed using a precision balance (Mettler Toledo, Switzerland) with the following masses recorded: 38.4658 g at 400°C, 19.2815 g at 500°C, and 19.3415 g at 600°C. The samples were then placed into a tubular furnace (Hefei crystal OTF-1200X, China) set to a heating rate of 10°C/min with a predefined temperature gradient. The carbonization process was maintained at constant temperatures of 400°C, 500°C, and 600°C for 2 h, followed by cooling to room temperature. The resultant carbon content was measured as follows: 13.0963 g at 400°C, 6.227 g at 500°C, and 5.9603 g at 600°C. A preliminary calculation indicated that the charcoal yield from rape straw powder is approximately one-third of the initial mass. Finally, the biochar was ground, sieved through a 100-mesh screen, bagged, and labeled as T400, T500, and T600, respectively.

2.1.3 Preparation of modified biochar

1) 5 g of biochar, prepared at different temperatures, was mixed with 1 mol/L KOH. The alkali-to-carbon ratios of biochar to KOH at 400°C were set to 0.5, 1.0, and 2.0, respectively. The mixture was stirred using a magnetic stirrer (Shanghai Shangyi, China) at 80°C and 100 r/mim for 1 h, followed by impregnation at room temperature for 10 h.

2) The mixture was filtered using a Buchner funnel, and the residue was baked in an oven at 60°C for 8 h.

3) The dried mixture was placed in a tubular furnace, heated to 600°C at a rate of 3°C/min under a nitrogen atmosphere, and activated for 30 min.

4) After cooling to room temperature, the activated biochar was washed with distilled water until neutral, then baked at 60°C for 8 h. The modified biochar was subsequently ground and sieved through a 100-mesh screen. The samples prepared with different alkali-to-carbon ratios were designated as AC0.5, AC1, and AC2.

2.2 Characterization of biochar

2.2.1 Elemental analysis

The contents of C, H, O, and N in the samples were determined using an elemental analyzer (2400 Ⅱ, Platinum Emmer, USA), and the H/C ratio was subsequently calculated.

2.2.2 Infrared spectroscopy

Four key parameters are provided by the infrared spectrum for analysis: peak number, peak position, peak shape, and peak intensity. Qualitative analysis is performed based on the characteristic absorption frequencies of functional groups. The number of peaks corresponds to the variety of functional groups present, while the peak intensity reflects the quantity of these groups[31].

The surface functional groups of the samples were characterized using Fourier transform infrared (FTIR) spectroscopy with an AA-6800 infrared spectrometer (Shimadzu, Japan). Trace amounts of the samples were placed into a mortar, followed by the addition of an appropriate amount of potassium bromide. After thorough grinding, the mixture was transferred to a tablet press to

form pellets, which were then analyzed using the infrared spectrometer.

2.2.3 Specific surface area and pore size analyses

Five samples were degassed for 6 h under a vacuum at 200°C, with the temperature maintained at 77 K using liquid nitrogen.

2.2.4 XRD analysis

X-ray diffraction (Bruker-8, Bruker Corporation, USA) was used to qualitatively analyze the crystal structure[32]. Experimental conditions: Cu Kα radiation was used as the excitation light source, with the X-ray tube operating at a current of 40 mA and a voltage of 40 kV. The scanning range was set to 2Θ: 2°-60°, with a scanning speed of 2°/min.

2.2.5 Raman spectroscopy analysis

The skeletal structure of the biochar samples was analyzed using a Raman spectrometer (Thermo Scientific, USA). The D and G peaks were utilized to assess the structural disorder of the sample, thereby determining its aromaticity[33]. The excitation wavelength was set at 532 nm, with a spectral range of 400-2800 cm^{-1}.

2.2.6 SEM analysis

The pore structure of the activated carbon was analyzed using scanning electron microscopy (SU8010, Hitachi, Japan). Scanning electron microscopy is distinguished by its large depth of field, which results in images with a pronounced three-dimensional appearance. The fracture morphology revealed by SEM reflects the material's fracture characteristics, leveraging the technique's deep depth of field. Additionally, the pore size distribution and surface roughness of the samples can be observed[34]. Microstructural images were captured at magnifications of 100×, 300×, 800×, 1000×, 3000×, 6000×, 10 000×, and 20 000×.

2.3 Single-factor experiment on the adsorption of biochar to tetracycline solution

2.3.1 Effects of varying pH values on biochar adsorption efficiency

50 mL of a 50 mg/L tetracycline solution were transferred into five 100 mL conical flasks. Subsequently, 0.3 g of biochar was added to each flask. The pH was then adjusted to 3, 5, 7, 9, and 11 using 0.1 mol/L hydrochloric acid and 5% sodium hydroxide solution, respectively. The flasks were labeled for later use. The five conical flasks were then placed in a 25°C water bath shaker and oscillated in the dark for 2 h before being removed. The resulting solutions were filtered using a suction filter. The absorbance of the filtrates was measured using a UV-spectrophotometer, based on the regression equation for tetracycline. Finally, the removal rate of tetracycline was calculated.

2.3.2 Effects of different biological carbon dosages on adsorption test

Sequentially add 50 mL of 50 mg/L tetracycline solution into four 100 mL conical flasks, followed by the addition of 0.2, 0.3, 0.5, and 0.6 g of biochar into each flask. Subsequently, place the flasks in a thermostatic oscillator set to 25°C and shake continuously for 2 h. After shaking, remove the flasks and filter the contents using an extraction filter. The absorbance of the filtrate was measured using a UV-spectrophotometer, and the concentration was determined based on the linear regression equation of the tetracycline solution. Finally, the removal rate was calculated using the appropriate formula.

2.3.3 Effects of different reaction time on biological carbon adsorption test

Add 50 mL of 50 mg/L tetracycline solution and 0.3 g of biochar to each of four 100 mL conical flasks. Subsequently, subject them to shaking at a constant temperature for 10, 30, 60, and 120 min, respectively. Afterward, remove the flasks. The filtrate is then extracted and filtered, and its absorbance is measured using a UV-spectrophotometer. The filtrate is then extracted and filtered, and its absorbance is measured using a UV-spectrophotometer.

2.3.4 Effect of different initial concentration on biochar adsorption test

Tetracycline solutions of 5 mg/L, 10 mg/L, 20 mg/L, 30 mg/L, and 50 mg/L were added to five separate 100 mL conical flasks, followed by the addition of 0.3 g of biochar to each flask. The conical flasks were then placed into a water bath thermostatic oscillator set at 25°C, oscillated at a constant temperature for 2 hours, and subsequently removed. The solutions were extracted and filtered using a suction filter. The absorbance of the filtrate was measured using a UV-spectrophotometer, and the concentration was determined based on the linear regression equation of the tetracycline solution. Finally, the removal rate (R) was calculated using the designated formula.

2.3.5 Orthogonal experiment on adsorption of tetracycline solution by biochar

Orthogonal comparison experiments were conducted using biochar dosage, adsorption time, and initial concentration of tetracycline solution as variables, with each factor having three levels. The biochar dosage levels were 0.2, 0.3, and 0.5 g. The adsorption time levels were 30, 60, and 120 min. The tetracycline solution concentration levels were 20, 30, and 50 mg/L.

2.3.6 Removal rate calculation

$$r = \frac{c_0 - c_t}{c_0} \times 100\% \quad (1)$$

where, c_0 is the initial concentration of tetracycline solution, mg/L; c_t is the residual concentration of tetracycline solution at t, mg/L; r is the removal rate of R-tetracycline solution, %.

2.4 Data analysis

All tests were conducted in triplicate, and the mean values were subsequently utilized. Analysis of variance (ANOVA) was employed to assess the significance of the results. Data calculations were performed using Excel, and graphs were generated with Origin (2018) and Visio.

3 Results and analysis

3.1 Elemental analysis

The contents of carbon (C), hydrogen (H), oxygen (O), and nitrogen (N) in biochar were determined using an elemental analyzer, and the H/C ratio was subsequently calculated. As listed in Table 1, with increasing pyrolysis temperature, the carbon (C) content rises, whereas the hydrogen (H) content decreases. This phenomenon primarily occurs because, at higher pyrolysis temperatures, the dehydration and decarboxylation reactions of lignin, cellulose, and hemicellulose are more pronounced. Consequently, oxygen is more likely to combine with hydrogen to form water molecules, leaving behind a higher concentration of carbon. The H/C ratio is commonly used to characterize the aromaticity of samples. A lower H/C ratio indicates greater aromaticity. In this experiment, the H/C ratio decreased with varying temperatures and alkaline-carbon ratios, indicating that polar groups on the biochar were pyrolytically removed from the carbon chain. This resulted in the formation of unsaturated or aromatic carbon ring structures, leading to a more condensed spatial structure, a higher degree of carbonization, and improved aromatic properties.

Table 1 The contents of different sample element

Sample	N/%	C/%	H/%	S/%	H/C
T400 AC0.5	6.23	56.50	5.372	0.335	0.0951
T400 AC1	6.07	56.33	5.319	0.334	0.0944
T400 AC2	5.67	56.15	5.264	0.330	0.0937
T500 AC0.5	6.24	66.67	5.303	0.335	0.0795
T600 AC0.5	6.23	69.45	5.289	0.371	0.0762

3.2 Infrared spectral analysis

Different functional groups influence the chemical properties of biochar's surface. Biochar prepared under varying conditions exhibits different functional groups. Figure 1 presents the infrared spectral analysis of the sample. The functional groups on the sample surface vary with different carbonization temperatures and alkali-carbon ratios. As shown in Figure 1, a prominent absorption peak appears near 3400 cm^{-1}, corresponding to the −OH vibration range of water. As the temperature of the activated carbon sample increases from 400°C to 600°C, the width of the stretching vibration peak for hydroxyl groups progressively decreases, along with a reduction in the phenolic hydroxyl groups. Notably, the sample pyrolyzed at 600°C demonstrates a significant enhancement in the dehydration reaction of rape straw-based porous biochar, leading to the loss of bound water and the rupture of hydrogen-bonded hydroxyl groups. These observations are consistent with the elemental analysis results. An evident absorption peak appears at 1400 cm^{-1}, with significantly increased vibration intensity as pyrolysis temperature rises. This indicates the presence of aromatic C=C bonds and CH bending vibrations. The biochar prepared at 400°C exhibits a well-developed aromatic structure. C=O bonds (aldehydes, ketones, and acids) appear at 1600 cm^{-1} and are prone to pyrolysis, resulting in liquid or gaseous byproducts. This process forms aromatic structures such as ketones and esters, thereby enhancing the surface complexation capacity of biochar. Under varying alkali-carbon ratios at 400°C, the vibration peaks of functional groups in biochar exhibit significant changes. The hydroxyl vibration peak of AC2 in the 3400 cm^{-1} range is relatively flat, whereas the peak strength for AC0.5 is pronounced. Based on the spectra, biochar with a higher number of surface functional groups has an increased number of active sites, which enhances its adsorption capacity.

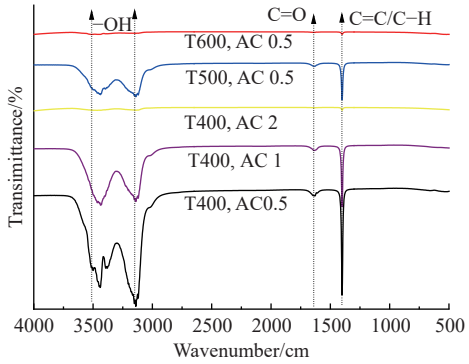

Figure 1 The infrared spectrum of the samples

3.3 Specific surface area and pore size analysis

Pyrolysis temperature and the alkali-carbon ratio significantly impact the surface structure of the biochar samples. The distribution of the specific surface area of the samples is shown above. According to Table 2, the specific surface area measured for T400 AC0.5 is the highest among the samples. Analysis of T400, T500, and T600 indicates that both the specific surface area and adsorption volume of biochar decrease significantly with increasing pyrolysis temperature, suggesting that the optimal specific surface area is achieved at 400°C. A greater number of active sites on the surface results in improved adsorption effectiveness. Consequently, this temperature represents the optimal condition for producing porous biochar from rapeseed straw. Figure 2 reveals that the sample exhibits a Type I isotherm, characterized by a hysteresis loop at high pressure. Hence, this indicates that the sample material possesses a microporous structure or exhibits monolayer adsorption, leading to strong adsorption performance. Notably, the curves for T400, AC1, and T400, AC2 are not fully closed. The possible explanations are as follows: 1) During nitrogen desorption, some nitrogen may remain trapped in the pores and not fully desorb, leading to incomplete curves; 2) The adsorption time may be insufficient, preventing the attainment of adsorption equilibrium.

Table 2 BET value

Samples	$S_{*BET}/m^2 \cdot g^{-1}$	$V^*/cm^3 \cdot g^{-1}$	D*/nm
T400 AC0.5	373.72	0.1753	1.8766
T400 AC1	28.43	0.0226	3.1323
T400 AC2	218.40	0.0972	1.7808
T500 AC0.5	357.38	0.1663	1.8608
T600 AC0.5	10.03	0.0183	7.2815

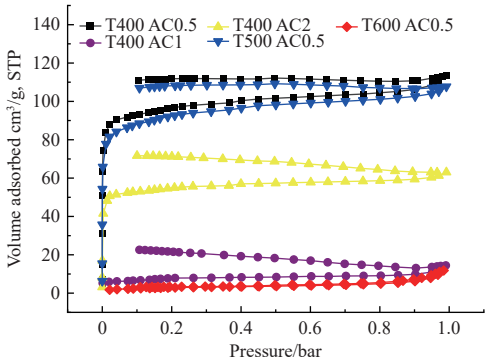

Figure 2 BET diagram

In summary, both the sample surface area and pore diameter decrease as pyrolysis temperature increases. Generally, the increase in pore volume and specific surface area results from the development of micropores due to the precipitation of volatile substances at higher pyrolysis temperatures. However, variations in the alkali-to-carbon ratio also impact pore size. Specifically, as the alkali-to-carbon ratio increases, the number of micropores decreases, leading to a gradual reduction in specific surface area.

3.4 XRD analysis

XRD analysis of the biochar samples revealed diffraction peaks at 28°, indicating the presence of a graphite carbon structure on the surface of the activated carbon. As illustrated in Figure 3, as the temperature increases from 400°C to 600°C, the diffraction peak shifts slightly to the right and its intensity decreases. This suggests that the liquefied material of the activated carbon sample reacts fully at 400°C. However, with further increases in pyrolysis temperature, the intensity of the characteristic peak decreases, indicating that the liquefied material does not fully react at 500°C and 600°C. This indicates that the graphite carbon content in the sample reaches its optimal level at a specific pyrolysis temperature. As the temperature continues to rise, the graphite content decreases, and the internal structure becomes disordered, with graphite carbon gradually transforming into non-graphitic carbon with an unstable structure. As shown in the figure, the XRD patterns of all five samples lack sharp absorption peaks, presenting a flat and smooth

profile, which indicates the absence of crystalline minerals in these samples. Comparing the sample spectra under isothermal conditions, at a pyrolysis temperature of 400°C and an alkali-to-carbon ratio of 0.5, the number of absorption peaks was more pronounced, and the diffraction peak was wider and stronger. As the alkali-to-carbon ratio increased, the intensity of the characteristic peak decreased, and the peak became narrower. Therefore, the XRD results indicate that the optimal alkali-to-carbon ratio for the biochar sample under isothermal conditions is 0.5.

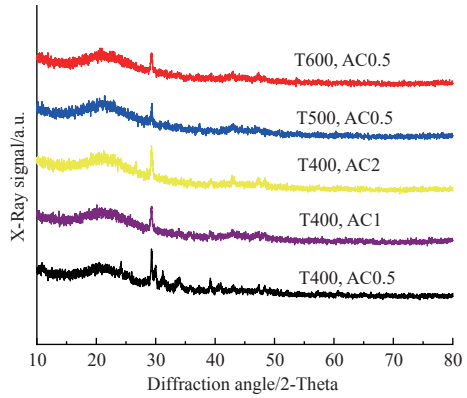

Figure 3 The XRD spectrum of the samples

3.5 Raman spectroscopy analysis

The microporous structures of the biochar samples were analyzed using Raman spectroscopy. All five samples exhibited saddle-like structures, indicative of their graphite-carbon composition. The D peak (1370 cm^{-1}) corresponds to disordered carbon, whereas the G peak (1560 cm^{-1}) corresponds to graphitized carbon. The intensity ratio of these two peaks indicates the degree of graphitization of the activated carbon samples. A higher ratio suggests lower graphitization and a less stable structure. Figure 4 illustrates the Raman spectra of activated carbon under various pyrolysis temperatures and alkali-carbon ratios. The increased D/G ratios observed at T400, T500, and T600 suggest an increase in disordered carbon crystals and a corresponding decrease in graphitization with rising temperature, which is consistent with the aforementioned XRD results. At T400, the D/G ratio of AC0.5 is the lowest, indicating minimal disordered carbon, maximum graphitization, strongest aromatization, and a stable structure. This suggests that T400 and AC0.5 represent the optimal conditions for carbon material preparation.

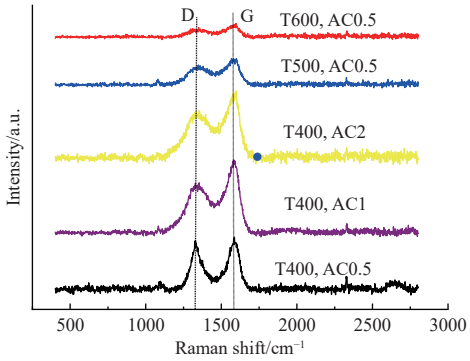

Figure 4 Raman spectroscopy of the sample

3.6 SEM analysis

According to the observations made using scanning electron microscopy, the surface structure and internal pore distribution of the biochar samples can be clearly visualized. The rape straw-based porous carbon material is composed of irregularly shaped curly sheets and large particles with a tubular structure. Figure 5 presents the results for five biochar samples. One of the most critical factors influencing adsorption is the pore structure. It can be observed from Figure 5 that all samples possess abundant pore structures, as shown in Figures 5a-5c, although there are some differences in pore size distribution. As illustrated in Figure 5d, the pore structure was severely damaged, and many pores were evidently blocked. Compared to the sample figure at 400°C, the pore structure of the sample subjected to high-temperature pyrolysis was irregular. This suggests that with increasing pyrolysis temperature, the collapse and shrinkage of pores in the biochar became severe, leading to significant pore damage and blockage. Figures 5a-5c show that under the condition of an isothermal alkali-carbon ratio of 0.5, the pore structure of the biochar samples was clear, with no debris blockage, and the pores were full. The abundant pore structure can provide a substantial number of adsorption sites for penetrating substances (molecules, ions, etc.), which is essential for the adsorption of heavy metal ions. Therefore, under isothermal conditions, an alkali-carbon ratio of 0.5 is the optimal condition for biochar preparation.

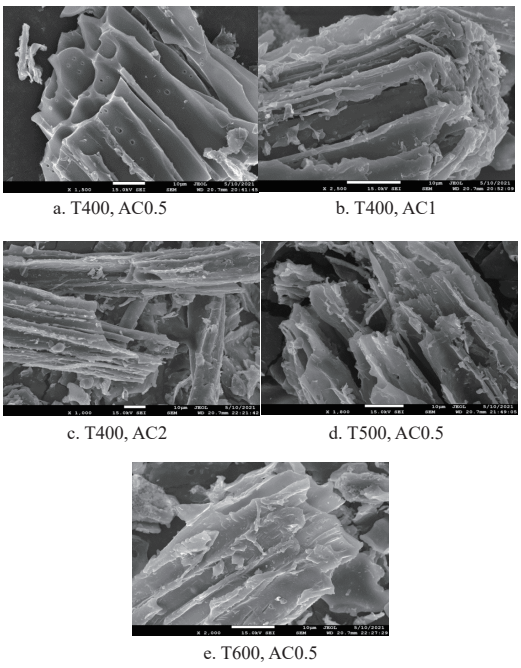

a. T400, AC0.5 b. T400, AC1

c. T400, AC2 d. T500, AC0.5

e. T600, AC0.5

Figure 5 The SEM analysis of the samples

3.7 Single factor adsorption effect of biochar on tetracycline solution

3.7.1 Effects of different pH values on biological carbon adsorption effect

The pH value can alter the state of tetracycline in the water environment and consequently affect its adsorption capacity. According to Figure 6, when the solution's pH was 3, the tetracycline removal rate was only 85.21%; when the pH ranged from 7 to 10, the removal rate increased; when the solution's pH was 11, the tetracycline removal rate reached 98.06%. As the pH value increased, the removal rate of tetracycline by biochar also increased. Neutral and alkaline conditions favor the adsorption of TCs. This finding is consistent with the experimental results of Li et al.[35] As the pH increased, the removal rate by rape carbon increased by 12.85%. However, two possible reasons may account for the deviation from the findings of Li et al.[36]

1) Differences in the pH values of raw materials.

2) Variations in pore volume and surface functional groups

resulted in more adsorption sites on the biochar surface.

3.7.2 Effects of different biological carbon dosages on adsorption effect

The dosage of biochar significantly impacted the removal rate of tetracycline in the organic solution. According to Figure 7, when the biochar dosage was 0.2 g, the removal rate of tetracycline was only 67.85%; at a biochar dosage of 0.6 g, the removal rate of tetracycline reached 98.25%, with the TCs concentration at its lowest. The efficiency of TCs removal increased with higher biochar dosages, which aligns with the findings of Yang et al.[37] As illustrated in Figure 7, the removal rates significantly varied between dosages of 0.2 g, 0.3 g, and 0.5 g. Therefore, 0.3 g was selected as the basic dosage in the followup experiment, and 0.2 g, 0.3 g, and 0.5 g were selected in the orthogonal experiment.

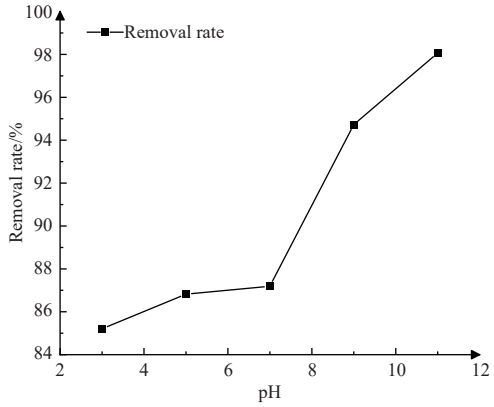

Figure 6 Influence of rice straw on removal rate

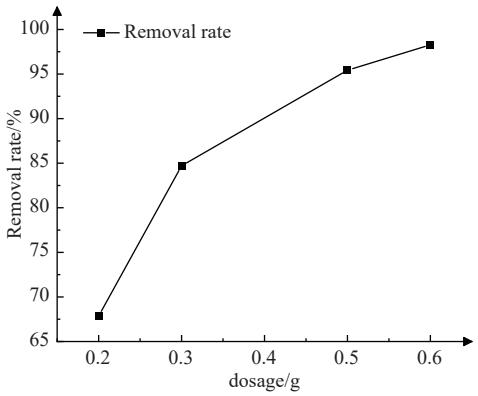

Figure 7 Influence of rice straw on removal rate

3.7.3 Effects of different reaction time on biological carbon adsorption effect

According to Figure 8, when the time was 10 min, the removal rate was only 73.88%. The change of tetracycline removal rate tended to be gentle between 10 min and 30 min, then gradually increased from 30 min to 60 min and reached the peak. After 60 min, the removal rate showed a downward trend, and the best reaction time was 60 min. The removal rate reached 91.8%. This is similar to the research results of Yang et al.[38], and different from Chen[39], the removal rate increases with the increase of time, it may be due to the high oscillation frequency during oscillation or the small initial concentration of the solution.

3.7.4 Effect of different initial concentration on biochar adsorption effect

The removal rate showed repeated changes in the adsorption test for different initial concentration of TCs. The removal rate increased with the increase of concentration between 5 mg/L and 20 mg/L, and decreased with increasing concentration between 20 mg/L and 50 mg/L. According to Figure 9, when the initial concentration was 20 mg/L, the removal rate was the best, reaching 93.94%.When the initial concentration was 50 mg/L, the removal rate was the lowest, only 84.72%. Therefore, 20 mg/L is the best initial concentration for this adsorption.

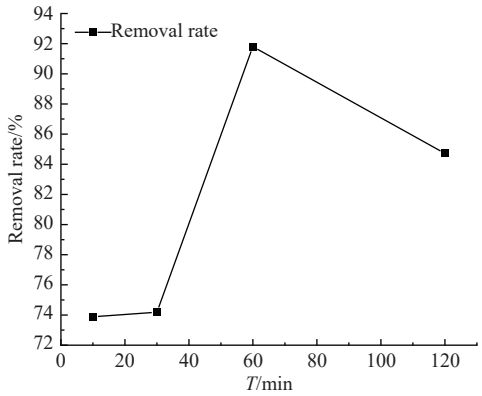

Figure 8 Effects of time on the remove rate

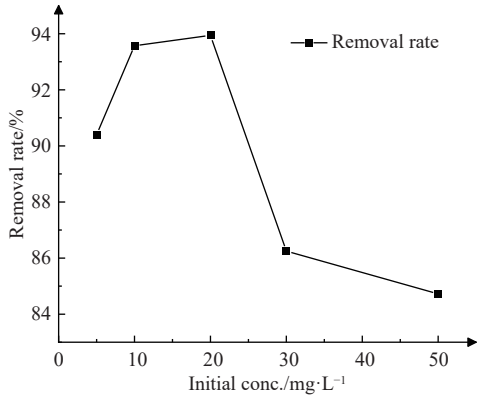

Figure 9 Effects of the initial concentration on the removal rate

3.7.5 Orthogonal experiment on adsorption of tetracycline solution by biochar

As listed in Table 3, the influence of the initial concentration of

Table 3 Orthogonal experimental results of tetracyclin organic solution of rape straw

Number	Experimental factors			
	Concentration/mg·L⁻¹	Dosage/g	Time/min	Results
	Different treatment level			
	A	B	C	Rate/%
X_1	20	0.20	30	95.07
X_2	20	0.30	60	97.54
X_3	20	0.50	120	90.63
X_4	30	0.20	60	98.53
X_5	30	0.30	120	86.25
X_6	30	0.50	30	90.67
X_7	50	0.20	120	67.85
X_8	50	0.30	30	73.88
X_9	50	0.50	60	92.54
I	283.24	261.45	259.62	
II	275.45	257.67	288.61	
III	234.27	273.84	244.73	
K_1	94.41	87.15	86.54	T=792.96
K_2	91.82	85.89	96.20	
K_3	78.09	91.28	81.58	
R	16.32	5.69	14.62	

TCs is greater than that of reaction time, which in turn is greater than that of biochar dosage. Therefore, the initial concentration of TCs is identified as the most significant factor influencing biochar adsorption, followed by reaction time, with biochar dosage being the least influential. A lower initial concentration of TCs leads to a higher conversion rate; hence, 20 mg/L is identified as the optimal concentration. The conversion rate peaked at a reaction time of 60 min. The removal rate was highest at a biochar dosage of 0.5 g. Consequently, the optimal combination identified in this study is A1B3C2.

4 Conclusions

With the increase of pyrolysis temperature and alkali-carbon ratio, the condensation effect of pyrolysis lead to the pore destruction and the decrease of adsorption volume. XRD results suggested the characteristic peak without any mineral crystal showed at 2Θ=28°, confirming the successful preparation of biochar. Besides, the intensity of characteristic peak of biochar decreased with the increase of pyrolysis temperature and alkali-carbon ratio, which reveals the increased internal disorder of biochar. The unsaturated aromatic structure and the oxygen-containing functional groups of rape straw biochar, such as -OH, C=C, C=O and C-H bonds, increased the surface-active sites. Raman spectroscopic analysis confirmed the saddle-like structure of prepared biochar.

The carbon content, specific surface area, pore volume, and pore structure of samples prepared at 400°C are superior to those prepared at other temperatures. The carbon and absorption peaks observed at an alkali-carbon ratio of 0.5 exhibit superior shapes compared to other ratios.

The rich pore structure and oxygen-containing functional groups of rape straw offer specific adsorption sites for permeable components (e.g., molecules, ions) in the porous carbon material, thereby creating the necessary conditions for the adsorption of organic solutions in wastewater. When using samples T400 and AC0.5 for the adsorption of tetracycline solution, the influencing factors in descending order were: initial concentration of tetracycline solution>adsorption reaction time>biochar dosage. The lower the initial concentration of TCs, the higher the conversion rate; hence, 20 mg/L is considered the optimal concentration. The conversion rate peaked at a reaction time of 60 min. The removal rate was maximized at a biochar dosage of 0.5 g, indicating that the optimal level for this study is A1B3C2.

Acknowledgements

This work was financially supported by the Key Research and Development Program of Shaanxi Province, China (Grant No. 2024NC-YBXM-258, 2023-YBNY-272), and the Scientific Research Project of City-University Co-construction of Shaanxi Province for State Key Laboratory of Qinba Bio-Resource and Ecological Environment (Grant No. SXC-2108, SXJ-2304).

[References]

[1] Cao Z, Wang S T, Luo P P, Xie D N, Zhu W. Watershed ecohydrological processes in a changing environment: Opportunities and challenges. Water, 2022; 14(9): 1502.

[2] Yang K, Wang Y Y, Ding A Z. Stability of biochar-remediated contaminated soil from a lead mine site. Journal of Agro-Environment Science, 2021; 40(12): 2715–2722. (in Chinese)

[3] Luo P P, Mu Y, Wang S T, Zhu W, Mishra B K, Huo A, et al. Exploring sustainable solutions for the water environment in Chinese and Southeast Asian cities. Ambio, 2022; 51(5): 1199–1218.

[4] Chen X P, Wang M, Yang C M, W L L. Review of contaminations in water of tetracyclines in China and toxicity on aquatic organisms. Applied Chemical Industry, 2021; 50(10): 2780–2785. (in Chinese)

[5] Lu X G, Xiao H Q, Wang H L, Zhang M H. Performance of magnetic $Mn_{0.02}Fe_{1.10}O_2$ CNT for tetracycline degradation by activation of persulfate and th emechanism analysis. Environmental Pollution and Control, 2021; 43(12): 1500–1505, 1512. (in Chinese)

[6] Zhan P, Zhu J H, Peng X M, Hu F P, Wang X Y, Long L L, et al. Removal of tetracycline from water by activation of persulfate with Fe, N co-doped mesoporous materials. Journal of Chemical Engineering of Chinese Universities, 2021; 35(6): 1090–1098. (in Chinese)

[7] Fan S S, Jin C J, Wen C, Zhao N N, Gu B M, Zhao Y G. Study on the treatment of tetracycline waste water by electro-activated sulfat. Journal of Ocean University of China (Natural Science), 2022; 52(1): 88–96. (in Chinese)

[8] Niu K L, Sun B, Liu Y, Zhu X M. Research progress of bismuth tungstate photocatalyst application in tetracycline wastewater treatment. Industrial Water Treatment, 2021; 41(11): 9–15. (in Chinese)

[9] Li M J, Luo W P. Current status of antibiotic contamination and research progress in removal methods. Leather Manufacture and Environmental Technology, 2021; 2(6): 77–78. (in Chinese)

[10] Almakki A, Jumas-Bilak E, Marchandin H, Licznar-Fajardo P. Antibiotic resistance in urban runoff. Science of The Total Environment, 2019; 667: 64–76.

[11] Costa L R d C, Féris L A. Use of functinalized adsorbents for tetracycline removal in wastewater: adsorption mechanism and comparison with activated carbon. Journal of Environmental Science and Health, 2020; 55(14): 1604–1614.

[12] He Y, Li X P, Li T T, Srinivasakannan C, Li S W, Yin S H, et al. Research progress on removal methods of Cl^- from industrial wastewater. Journal of Environmental Chemical Engineering, 2023; 11(1): 109163.

[13] Liu J F, Lin H, He Y H, Dong Y B, Menzembere E R G Y. Novel CoS2/MoS2@Zeolite with excellent adsorption and photocatalytic performance for tetracycline removal in simulated wastewater. Journal of Cleaner Production, 2020; 260: 121047.

[14] Liang J Z, Xu W C, Lai S F, Xiao K B, Wu X L, Li F H, et al. Research progress on preparation and peroxymonosulfate activation of magnetic biochar. Environmental Chemistry, 2021; 40(9): 2901–2911. (in Chinese)

[15] Krajčovičová T E, Hatala M, Gemeiner P, Híveš J, Mackuľak T, Nemčeková K, et al. Biochar for water pollution control: From sensing to decontamination. Chemosensors, 2023; 11: 394.

[16] Sun C. Modified biochars for heavy metal and organic pollutant removal: performance and mechanism. PhD dissertation. Hangzhou: Zhejiang University, 2021; 157p. (in Chinese)

[17] Michael I, Rizzo L, McArdell C S, Manaia C M, Merlin C, Schwartz T, et al. Urban wastewater treatment plants as hotspots for the release of antibiotics in the environment: A review. Water Research, 2013; 47(3): 957–995.

[18] Zhou L, Zhang G H, Zeng Y L, Bao X L, Liu B, Cheng L. Endogenous iron-enriched biochar derived from steel mill wastewater sludge for tetracycline removal: Heavy metals stabilization, adsorption performance and mechanism. Chemosphere, 2024; 359: 142263.

[19] Dong C, Li M P, Guo C X, Wei L G. The influence of modifying methods on the adsorption of methylene blue by *Moringa ole ifera* seed shelling biochar. Food & Machinery, 2021; 37(11): 12–18. (in Chinese)

[20] Wang X J, Nian F Z, Xia Y S, Jiang X Y, Liu R R, Zhao Y X, et al. Current status of antibiotic use and its behavior in ecological system. Soil and Fertilizer Sciences in China, 2020; 6: 286–292. (in Chinese)

[21] Sheng D H, Ying X T, Li R, Cheng S Y, Zhang C, Dong W, et al. Polydopamine-mediated modification of ZIF-8 onto magnetic nanoparticles for enhanced tetracycline adsorption from wastewater. Chemosphere, 2022; 308: 136249.

[22] Zhang Q R, Ji L Y, Gao C C, Lv H H, Sik-Ok Y. Preparation of modified biochar and its application in environmental remediation. Journal of Agro-Environment Science, 2021; 40(5): 913–925. (in Chinese)

[23] Li D W, Tian Y Y, Hao J H, Tian B, Li J H, Che Y J. Preparation of N-doped ultramicropore-containing active carbons from waste soybean dreg by one-step carbonization/activation. Transactions of the CSAE, 2015; 31(19): 309–314. (in Chinese)

[24] Wang Y Y. Preparation, modification and adsorption to Cd^{2+} of activated carbons. MS dissertation. Urumchi: Xinjiang University, 2016; 67p. (in Chinese)

[25] Cheng L L. The comparison research of biochar adsorption performance by KOH activation method. MS dissertation. Dalian: Dalian Maritime University, 2017; 78p. (in Chinese)
[26] Yan L L, Song X, Miao J W, Ma Y F, Zhao T, Yin M Y. Removal of tetracycline from water by adsorption with biochar: A review. Journal of Water Process Engineering, 2024; 60: 105215.
[27] Li G T, Li K L, Zhang S Y, Liu Y X, Wang N, Tan Y F. Adsorption of methylene blue and tetracycline on lignocellulosic biochar. Jiangsu Agricultural Sciences, 2021; 49(18): 234–240. (in Chinese)
[28] Huang C H, Stone A T. Hydrolysis of naptalam and structurally related amides: Inhibition by dissolved metal ions and metal (Hydr) oxide surfaces. Journal of Agricultural and Food Chemistry, 1999; 47(10): 4425–4434.
[29] Santás-Miguel V, Fernández-Sanjurjo M J, Núñez-Delgado A, Álvarez-Rodríguez E, Díaz-Raviña M; Arias-Estévez M, et al. Use of biomass ash to reduce toxicity affecting soil bacterial community growth due to tetracycline antibiotics. Journal of Environmental Management, 2020; 269: 110838.
[30] Wang L Y, Xie X. Progress in preparation and application of biochar. Agriculture and Technology, 2020; 40(22): 34–36. (in Chinese)
[31] Gao C X, Lan Y, Zhan Y W, Li Y C, Jiang J Q, Li Y Q, et al. Preparation of porous biochar from fusarium wilt-infected banana straw for remediation of cadmium pollution in water bodies. Scientific Reports, 2024; 14: 13821.
[32] Wang T. Sorption of carbendazim in solution by activated carbon prepared from rape straw and its mechanism. MS dissertation. Wuhan: Huazhong Agricultural University, 2018; 78p. (in Chinese)
[33] Pan M. Biochar adsorption of antibiotics and its implications to remediation of contaminated soil. Water Air Soil Pollut, 2020; 231: 221.
[34] Zhong X X, Wang T, Wang K, Gao R L, Yue X L, Liu Y H, et al. Impacts of phosphorus acid concentration and pyrolysis temperature on structure and property of biochar. Journal of Natural Science of Hunan Normal University, 2018; 41(1): 48–53. (in Chinese)
[35] Li J J. Study on the adsorption of tetracycline in aqueous solution by modified biochar. MS dissertation. Harbin: Northeast Agricultural University, 2020; 78p. (in Chinese)
[36] Li Y X, Wang M J, Luan R J, Zhang Y Q, Zhang S, Qi Z C. Adsorption of tetracycline onto biochars under different solution chemistry conditions. Chemical Research, 2021; 32(6): 494–500. (in Chinese)
[37] Yang Q L. Preparation of corn straw based porous carbon and its adsorption properties for tetracycline in water. MS dissertation. Guangzhou: South China University of Technology, 2020; 92p. (in Chinese)
[38] Yang Q L, Wu P X. Preparation of modified porous biochar and its adsorption properties for tetracycline in water. Acta Scientiae Circumstantiae, 2019; 39(12): 3973–3984. (in Chinese)
[39] Chen T W. The characteristics of biochars derived from rice straw and swine manure and their adsorption properties for tetracycline. MS dissertation. Ya'an: Sichuan Agricultural University, 2019; 62p. (in Chinese)